

## First Structural Investigation of a Super-Hydrated Zeolite

Yongjae Lee,<sup>§,†,‡</sup> Joseph A. Hriljac,<sup>†</sup> Thomas Vogt,<sup>‡</sup>  
John B. Parise,<sup>\*,§</sup> and Gilberto Artioli<sup>||</sup>

Geosciences Department, State University of New York  
Stony Brook, New York 11794-2100

School of Chemical Sciences, The University of Birmingham  
Birmingham, B15 2TT, UK

Physics Department, Brookhaven National Laboratory  
Upton New York 11973-5000

University of Milan  
Dipartimento Scienze Terra, I-20133, Milan, Italy

Received September 17, 2001

Pressure and temperature are basic thermodynamic variables transforming matter from one state to another. Our knowledge of pressure-induced phase transformations of zeolites, however, is very limited compared to the vast number of temperature-dependent studies performed over the past several decades.<sup>1–3</sup> This is partly due to the required experimental complexities as well as the analytical ambiguities arising from the porous nature of the materials, which can lead to compositional changes upon interaction with various pressure-transmitting media.<sup>4–6</sup>

The large variety of zeolite structures is due to the numerous possible linkages of (Al,SiO<sub>4</sub>)-tetrahedra that bound nanopores of various sizes. The built-in flexibility allows these structures to contract and expand in response to external changes and alters the chemistry occurring in the nanopores. Unusual effects such as negative thermal expansion and cation relocations in zeolite rho have recently been recognized to be driven by temperature-induced chemical changes.<sup>7</sup> Therefore, applying external hydrostatic pressure was also anticipated to alter the chemical environment within the pores. We have reported different phase transitions depending on the type of cations residing inside the pores in zeolite rho.<sup>8</sup> Various interaction schemes between cation and pressure-transmitting media have been proposed to drive the observed phase transitions in rho and other zeolites,<sup>8–10</sup> but no structural evidence for these pressure-induced chemical changes has been reported to date.

We have measured powder diffraction data of natrolite<sup>11</sup> as a function of pressure up to 5.0 GPa using a diamond-anvil cell (DAC) and a 200 μm-focused monochromatic synchrotron X-ray beam.<sup>12</sup> Upon pressure increase, there is an abrupt volume expansion (ca. 2.5%) between 0.8 and 1.5 GPa. Rietveld refinements using these data showed that this anomalous swelling is due to

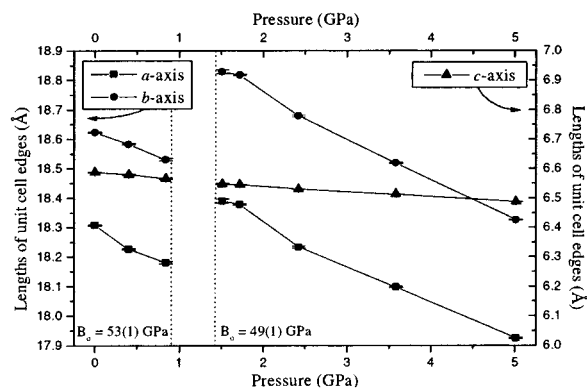


**Figure 1.** Changes in the unit cell edge lengths (Å) of natrolite as a function of pressure. Esd's are multiplied by three at each point. The structure model at ambient pressure is from the work of Baur et al.<sup>15</sup>

the selective sorption of water from the alcohol-based pressure-transmitting media into the expanded channels, which gives rise to a “super-hydrated” phase of natrolite, Na<sub>16</sub>Al<sub>16</sub>Si<sub>24</sub>O<sub>80</sub>·32H<sub>2</sub>O, distinct from the normal natrolite, Na<sub>16</sub>Al<sub>16</sub>Si<sub>24</sub>O<sub>80</sub>·16H<sub>2</sub>O, at ambient conditions.

The evolution of the unit cell parameters of natrolite is shown as a function of pressure in Figure 1. Between 0.8 and 1.5 GPa,

(11) The natrolite framework is composed of 4-1 T<sub>5</sub>O<sub>10</sub> tetrahedral building units that are connected along the *c*-axis forming the so-called natrolite chains. The mode of linkage between the chains<sup>13</sup> produces helical eight-ring channels along the *c*-axis with T<sub>10</sub>O<sub>20</sub> windows intersecting perpendicular to the channel. Under ambient conditions, the aluminosilicate natrolite has an ordered distribution of Al and Si over the T-sites in *Fdd2* (orthorhombic) symmetry with sodium cations along the channels and water molecules close to the T<sub>10</sub>O<sub>20</sub> windows.<sup>14</sup> The flexible linkages between and within the chains and their interaction with stuffed cations and waters give rise to various structural distortions, depending on the composition and temperatures.<sup>15–17</sup> A distortion parameter,  $\psi$ , which measures the average angle between the 4-1 building unit and the *a*- and *b*-axes, can describe the degree of the chain rotation.<sup>18</sup> Belitsky et al. have reported that under high water pressures, natrolite undergoes a phase transition with a corresponding volume increase.<sup>10</sup> With this change, there is also an increase in the water self-diffusion as measured by NMR.<sup>19</sup> It has been proposed, but no direct evidence given, that these changes are due to the incorporation of extra water into the pores.

(12) High-pressure experimental details of the X7A beamline of the National Synchrotron Light Source (NSLS) are described elsewhere.<sup>8</sup> Powdered sample of mineral natrolite (from Dutoitspan, South Africa, EPMA: Na<sub>16</sub>Al<sub>16</sub>Si<sub>24</sub>O<sub>80</sub>·16H<sub>2</sub>O)<sup>20</sup> was loaded into a 200 μm diameter sample chamber in a pre-indented Inconel gasket, along with a few small ruby chips as a pressure gauge. Initial experiments using water as a pressure transmission medium led to broadened diffraction lines, probably due to the solidification of water above 1.0 GPa. A mixture of 16:3:1 by volume of methanol:ethanol:water was thereafter used as a pressure medium (hydrostatic to above 10 GPa).<sup>21</sup> The pressure at the sample was measured by detecting the shift in the R1 emission line of the included ruby chips. No evidence of nonhydrostatic conditions or pressure anisotropy was detected during our experiments. Typically, the sample was equilibrated for about 15 min at each measured pressure, and the diffraction data were collected for 3–5 h (3–35° 2θ, λ = 0.7054 Å) using a gas-proportional position-sensitive detector. The sample pressure was raised by 0.5–1.0 GPa increments before subsequent data measurements up to 5 GPa, where the DAC failed due to the accidental breakage of a diamond. There was no evidence of stress-induced peak broadening or pressure-driven amorphization and the recovered sample maintained its original white color, with its cell parameters similar to those at ambient conditions (within 3σ). Bulk moduli were calculated by fitting Murnaghan equation of states to normalized volumes.

(13) Smith, J. V. Z. *Kristallogr.* **1983**, *165*, 191.

(14) Meier, W. M. Z. *Kristallogr.* **1960**, *113*, 430.

(15) Baur, W. H.; Kassner, D.; Kim, C.-H.; Sieber, N. H. *Eur. J. Mineral.* **1990**, *2*, 761.

(16) Alberti, A.; Cruciani, G.; Dauri, I. *Eur. J. Mineral.* **1995**, *7*, 501.

(17) Lee, Y.; Kim, S. J.; Parise, J. B. *Microporous Mesoporous Mater.* **2000**, *34*, 255.

(18) Alberti, A.; Vezzalini, G. *Acta Crystallogr.* **1981**, *B37*, 781.

(19) Moroz, N. K.; Kholopov, E. V.; Belitsky, I. A.; Fursenko, B. A. *Microporous Mesoporous Mater.* **2001**, *42*, 113.

(20) Artioli, G.; Smith, J. V.; Kwick, A. *Acta Crystallogr.* **1984**, *C40*, 1658.

(21) Hazen, R. M.; Finger, L. W. *Comparative Crystal Chemistry*; John Wiley & Sons: New York, 1982.

<sup>§</sup> Geosciences Department, State University of New York.

<sup>†</sup> School of Chemical Sciences, The University of Birmingham.

<sup>‡</sup> Physics Department, Brookhaven National Laboratory.

<sup>||</sup> University of Milan, Dipartimento Scienze Terra.

<sup>†</sup> Present address: Physics Dept., BNL, Upton, NY.

(1) Corbin, D. R.; Abrams, L.; Jones, G. A.; Eddy, M. M.; Harrison, W. T. A.; Stucky, G. D.; Cox, D. E. *J. Am. Chem. Soc.* **1990**, *112*, 4821.

(2) Baur, W. H.; Joswig, W. *Neues Jahrb. Mineral., Monatsh.* **1996**, 171–187.

(3) Artioli, G. In *In situ structural and kinetic powder diffraction studies of aluminosilicates*; Wright, K., Catlow, R., Eds.; Kluwer: Dordrecht, 1999; NATO Sciences Series, Series C, Vol. 543, pp 177–187.

(4) Hazen, R. M. *Science* **1983**, *219*, 1065.

(5) Knorr, K.; Braunbarth, C. M.; van de Goor, G.; Behrens, P.; Griewatsch, C.; Depmeier, W. *Solid State Commun.* **2000**, *113*, 503.

(6) Rutter, M. D.; Uchida, T.; Secco, R. A.; Huang, Y.; Wang, Y. *J. Phys. Chem. Solids* **2001**, *62*, 599.

(7) Lee, Y.; Reissner, B. A.; Hanson, J. C.; Jones, G. A.; Parise, J. B.; Corbin, D. R.; Toby, B. H.; Freitag, A.; Larese, J. Z.; Kahlenberg, V. *J. Phys. Chem. B* **2001**, *105*, 7188.

(8) Lee, Y.; Hriljac, J. A.; Vogt, T.; Parise, J. B.; Edmondson, M. J.; Anderson, P. A.; Corbin, D. R.; Nagai, T. *J. Am. Chem. Soc.* **2001**, *123*, 8418.

(9) Hazen, R. M.; Finger, L. W. *J. Appl. Phys.* **1984**, *56*, 1838–1840.

(10) Belitsky, I. A.; Fursenko, B. A.; Gubada, S. P.; Kholdeev, O. V.; Seryotkin, Y. V. *Phys. Chem. Miner.* **1992**, *18*, 497.

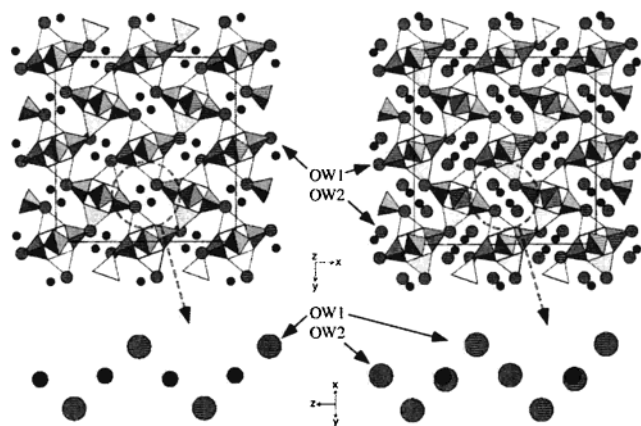


**Figure 2.** Polyhedral representations of natrolite at 0.40 GPa (left) and at 1.51 GPa (right) viewed along [001], the chain/channel axis. Large-light circles represent water molecules; small-dark ones, sodium cations. Chains of water and sodium are viewed along [110] below each model. Dark (light) tetrahedra illustrate an ordered distribution of Si (Al) atoms in the framework. Straight lines define the unit cell.

the pressure-induced swelling is caused by the expansion of the unit cell along the  $a$ - and  $b$ -axes, whereas the  $c$ -axis shows the expected contraction behavior throughout the volume expansion period. This anisotropic swelling suggests that the rotation of the chains along the  $c$ -axis and subsequent expansion of the channels in the (001) plane is responsible for the observed volume increase. The calculated bulk modulus of the large-volume natrolite ( $B_0 = 49(1)$  GPa) is slightly smaller than that of the normal natrolite ( $B_0 = 53(1)$  GPa), illustrating increased compressibility for this high-water-content phase.

The changes in the crystal structure accompanying the pressure-induced swelling were investigated by performing Rietveld refinements<sup>22</sup> using the framework geometrical constraints and the diffraction data collected in the pressure range examined. The two structural models for the phases before and after the volume expansion are shown in Figure 2. As the pressure increases up to 0.8 GPa, the water molecules shift away from the center of the  $T_{10}O_{20}$  window, close to one of the bridging O(2) oxygens, resulting in an increase of the coordination number for the OW1 water from four (2 Na + 2 O) at 0.4 GPa to five (2 Na + 3 O) at 0.8 GPa. Considering only the extraframework species, the water molecules and the sodium cations bond to form an infinite chain along the  $c$ -axis (Figure 2, left). After the volume expansion at 1.5 GPa, an additional fully occupied water site (OW2) appears along the channel, leading to 32  $H_2O$  per unit cell. This new site has been proposed to be half-filled with water molecules in paranatrolite (24  $H_2O$  per unit cell),<sup>25,26</sup> which gave rise to an anomalous increase in water mobility in NMR and other spectroscopic measurements.<sup>19,27</sup> In fact, we have observed a peak splitting in the powder diffraction pattern at 1.25 GPa. We suspect

(22) Rietveld structure refinements were performed using the GSAS suite of programs.<sup>23</sup> The starting framework model at each pressure point was constructed from DLS-minimization,<sup>24</sup> which was later constrained during the refinement process. Difference Fourier maps were generated, and sodium and oxygen atoms were used to model the extraframework species (Na cations and water molecules, respectively). Refinement of the fractional site occupancies indicated that these atoms fully occupy the extraframework sites, which were later fixed to unity. An overall isotropic displacement parameter was used for the framework atoms; another was used for the nonframework oxygens and cations.

(23) Larson, A. C.; Von Dreele, R. B. "GSAS: General Structure Analysis System," Report LAUR 86-748, Los Alamos National Laboratory: New Mexico, 1986.

(24) Meier, W. H.; Villiger, H. Z. *Kristallogr.* **1969**, *129*, 411.

(25) Chao, G. Y. *Can. Mineral.* **1980**, *18*, 85.

(26) Baur, W. H. *Cryst. Res. Technol.* **1991**, *26*, 169.

(27) Gabuda, S. P.; Kozlova, S. G. *J. Struct. Chem.* **1997**, *38*, 562.

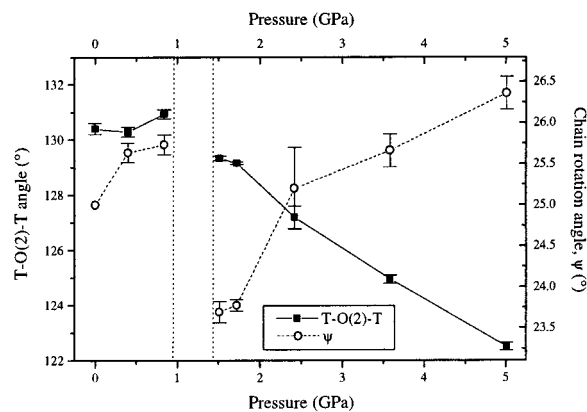


**Figure 3.** Changes in T-O(2)-T bond angle and overall chain rotation angle of natrolite as a function of pressure.

that at this pressure a pseudo-orthorhombic paranatrolite (with disordered water sublattice) or its mixture with the super-hydrated orthorhombic natrolite is present. Future work is in progress to clarify this. The water molecule at the OW2 site is coordinated by one sodium cation and six framework oxygens, forming a distorted capped trigonal prism, whereas the OW1 water moves back to the center of the  $T_{10}O_{20}$  window in a distorted tetrahedral environment. In addition, unlike the chain of sodium and water in the low-pressure phase below 0.8 GPa, the superhydration at the OW2 site generates an infinite chain of hydrogen-bonded waters along the  $c$ -axis with O-O distances between 2.80(4) and 3.09(4) Å (Figure 2, right). The position of the sodium cation does not show any appreciable changes throughout the superhydration region.

The changes in the framework geometry during the volume expansion and the superhydration processes can be monitored using the T-O-T bond angles within and between the chains. The T-O-T angles within the chain do not follow any systematic changes, whereas the bridging T-O(2)-T angle between the chains shows small changes before, and a continuous contraction after the superhydration, respectively. Coupled with this, the overall chain rotation angle,  $\psi$ , increases initially up to 25.7° at 0.8 GPa, drops to 23.7° during superhydration, and increases back up to 5.0 GPa (Figure 3). This indicates that superhydration is coupled to the relaxation of the overall distortion of the framework by expanding the pore space perpendicular to the channel.

More detailed structural changes of super-hydrated natrolite upon pressure release are unclear, as are those that occur during the volume expansion. Diffraction data on the recovered sample, however, suggest the reversibility of the system. We intend to clarify these issues in a follow-up study. Pressure-induced hydration (or other chemical changes) in other members of fibrous zeolites will also be monitored using synchrotron X-ray high-pressure diffraction.

**Acknowledgment.** This work was supported by the NSF (DMR-0095633) and an LDRD from BNL. Y.L. is grateful for support from an ACS-PRF grant to pursue high-pressure studies. Research carried out in part at the NSLS at BNL is supported by the U.S. DoE, Division of Materials Sciences and Division of Chemical Sciences (DE-Ac02-98CH10886 for beamline X7A). We acknowledge the Geophysical Lab of the Carnegie Institute for allowing us the use of the ruby laser system of beamline X17C.

**Supporting Information Available:** Selected refinement results (PDF). This material is available free of charge via the Internet at <http://pubs.acs.org>.